Electronic Supplementary Material (ESI) for ChemComm.

Supporting Information

Investigating the Role of Zinc Precursor during the Synthesis of the Core of III-V QDs

Yujin Kim[a]* and Seonghoon Lee[a]

[a] School of Chemistry, Seoul National University, Seoul 08826, Republic of Korea.

Email address: yjkim0921@snu.ac.kr

Experimental

Materials and methods

Materials.

Indium chloride ($InCl_3$, 99.999%) and gallium chloride ($GaCl_3$, 99.999%) were purchased from Strem Chemicals. Zinc chloride ($ZnCl_2$, 98%) were purchased from Samchun. Tris(trimethylsilyl)phosphine ($P(TMS)_3$, 95%) was purchased from JSI Silicone Co. Manganese(II) chloride ($MnCl_2$, 99.99%), calcium chloride ($CaCl_2$, 96%), 1-octadecene (ODE, 90%), sulfur (S, 99.98%), oleylamine (OLA, 70%), 1-dodecanethiol (DDT, 98%), and trioctylphosphine (TOP, 90%) were obtained from Aldrich. All the chemicals were used as received.

Preparation of complexes and P precursor

In-TOP, Ga-TOP, Zn-TOP stock solutions. All three stock solutions were prepared as mentioned in our previous paper.[1]

Ca-TOP and Mn-TOP stock solutions. To prepare the Ca-TOP stock solution, 1.25 mmol $CaCl_2$ and 1.25 mmol $MnCl_2$ were dissolved in 2.2 mL TOP each and magnetically stirred at room temperature overnight.

$HP(TMS)_2$ solution. As introduced in our previous paper, 1 mL $P(TMS)_3$ (0.5M in ODE) solution was mixed with 0.28 mL OLA.

Synthesis procedures of the cores

The core is synthesized following the method mentioned in our previous paper. The procedure is slightly modified where additional metal-TOP complex besides In-TOP and Ga-TOP complex precursors was added in the step of core synthesis. The flask with 8mL ODE was prepared after degassing and backfilling with N_2. Then, 0.03 mL In-TOP, 0.21 mL Ga-TOP, and additional metal precursors were injected into the flask and heated to 190 °C. At this temperature, prepared 1.28 mL of $HP(TMS)_2$ solution was quickly injected. The solution was stirred at the injection temperature for 15 min. After 15 min of the growth time, the solution was quickly cooled down to the room temperature. The resultant core solution was purified with ethanol and then re-dispersed in hexane for further use.

Characterization of the cores

Optical characterization. The UV-vis absorption spectra were measured using an Agilent Cary 5000 UV-vis-NIR spectrometer. The PL spectra were obtained using the ACTON SpectraPro 2350i spectrometer.

TEM. The TEM images were acquired using a JEOL JEM-F200 instrument with accelerating voltage of 200 kV using the samples prepared by dropping the diluted solution in hexane on a cooper grid (300 mesh) coated with a carbon film. The obtained images were used to determine the size using ImageJ program which measures the sizes in accordance with the scale bar.

ICP-AES. The ICP-AES spectra were plotted using the data obtained from the OPTIMA 8300 instrument. The samples were prepared by dissolving the core in an aqua regia solution after purifying the core with ethanol 10 times and then drying the precipitates overnight in a vacuum oven. The spectra were used to explicate the composition of the core.

Powder XRD. The XRD patterns were obtained using a New D8 Advanced (Bruker) system with Cu-Ka radiation (1.54 Å). The organic coordinating ligands were removed *via* multiple purification steps with ethanol for the sample preparation.

XPS. XPS analysis has been performed using AXIS-NOVA (Kratos) with a monochromatic Al Ka photon

source (1486.6 eV). The sample has prepared by spin-coating the solution in hexane on Si-wafer at a spin rate of 1000 rpm for 20s.

Absolute hardness of materials

Trioctylphosphine is harder than $HP(TMS)_2$. According to Pearson, absolute hardness is defined as the difference between ionization potential and electron affinity divided by 2. Hard molecules have a large HOMO-LUMO gap and high polarizability. For example, based on Pearson's absolute hardness scale, among three different molecules, PF_3, PH_3, and $P(CH_3)_3$, PF_3 is the hardest molecule and $P(CH_3)_3$ is the softest molecule. This is because -F has a greater electronegativity than P so that -F withdraws the electrons away from P. On the other hand, $-CH_3$ is the electron-donating group. Different absolute hardnesses of these three molecules are due to the electron-withdrawing characteristic of -F and the electron-donating characteristic of $-CH_3$. Likewise, the hardness of TOP and $HP(TMS)_2$ can be speculated. TOP has three $-C_8H_{17}$ groups around P and $HP(TMS)_2$ has one -H and two $-Si(CH_3)_3$ groups. Three $-C_8H_{17}$ are electron-withdrawing groups and $-Si(CH_3)_3$ groups. Electronegativity of P is greater than that of Si so that P withdraws electrons. Since $-Si(CH_3)_3$ is more electron-withdrawing than $-C_8H_{17}$, we can conclude that TOP is harder than $HP(TMS)_2$.

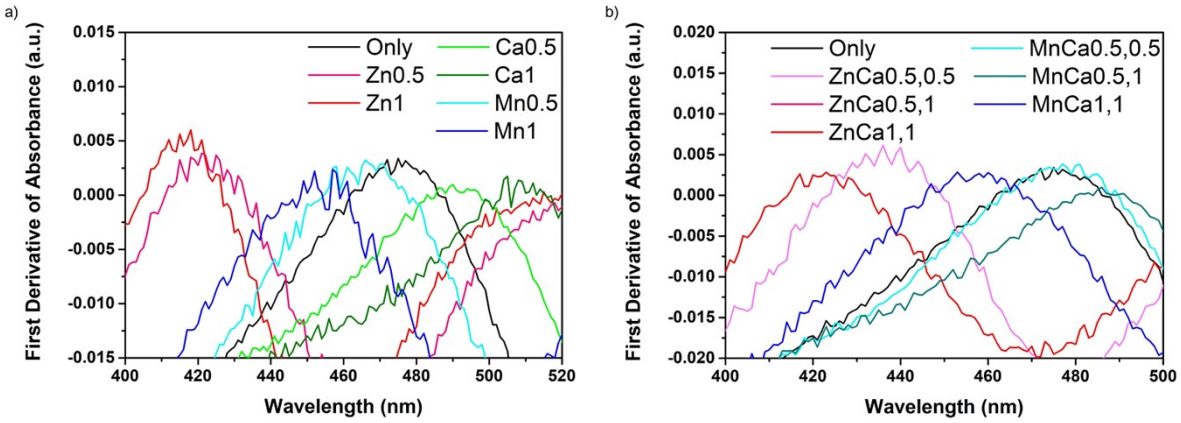

Fig. S1. The spectra of first derivatives of the absorption spectra: (a) Only sample and single metal samples and (b) two metal samples

Theoretical Analysis

There are two cases when the dopants are introduced into the system. One is that the dopant is assimilated to the intrinsic semiconductor forming alloy. In this case, the change in exciton energy will follow the Vegard's rule. Another case is that the dopant insists on maintaining its own identity so that its energy states are formed within the energy states of intrinsic material. In this case, if energy states exist within the band gap of parent material, the photoluminescence caused by the transition state of dopant will appear. If energy states of dopants exist in the bands of parent material, no change will be observed.

Manganese ion has been used as dopant in numerous types of nanocrystals.[2,3] Based on atomic spectra database from National Institute of Standards and Technology (NIST),[4] the first transition from the ground state to the first excited state of Mn^{2+} ion requires approximately 26,824 cm^{-1} (~ 400 nm) of energy. This transition is corresponding to d-d transition when ion is by itself and the position of energy levels is affected by the surroundings. When Mn^{2+} is doped in InGaP, Mn^{2+} is encircled by phosphorus in tetrahedral coordination. Zhang *et al.* demonstrated that the transition of Mn^{2+} in tetrahedral coordination emitted the orange color (~ 590 nm).[5] If Mn^{2+} has been doped in the core, the energy levels of Mn^{2+} dopant would exist within the exciton energy of Only sample or would induce the decrease in the exciton energy following Vegard's rule. Thus, the doping of Mn^{2+} would have resulted in either red-shift or another transition state approximately at 590 nm. However, neither phenomenon has been perceived with Mn samples. Based on the experiment data and theoretical analysis, it could be settled that Mn^{2+} used in the synthesis has not been doped in the core.

Similarly, the transition from the ground state to the first excited state of Ca^{2+} ion has been investigated. According to the NIST database, the first transition of Ca^{2+} by itself requires 203,373 cm^{-1} (~ 49 nm) of energy. Compared to the first transition of Mn^{2+}, the transition of Ca^{2+} demands huge amount of energy because it is the transition from 3p orbital to 4s orbital. This energy states do not exist within the band gap of InGaP so that the states would exist in the bands of InGaP, valence band and conduction band. If Ca^{2+} has been doped in the core and assimilated with InGaP material, blue-shift of the core might have been observed. Moreover, if Ca^{2+} has insisted on having its own characteristic while doped, no change would have been caused besides adding its own energy states in the bands of InGaP. Nevertheless, red-shift and the increase in the ratio of Ga to In have been identified. Thus, it can be determined that calcium ion has not been doped in the core. Lastly, atomic spectra of Zn^{2+} ion shows that the first transition state takes place from 3d orbital to 4s orbital requiring approximately 78,000 cm^{-1} (~ 128 nm) of energy. The energy levels of Zn^{2+} ion in the phosphorus cage of InGaP will be shifted like the energy states of Mn^{2+}. For example, when zinc was doped in CsBr perovskite quantum dots, the absorption peaks caused by the energy states of Zn^{2+} ion appeared at 381nm and 404nm.[6] Therefore, in InGaP system, the energy states of Zn^{2+} ion would exist in each bands. If Zn^{2+} has been doped, it would have caused blue-shift of the core or no change besides adding its own energy states. However, since it was confirmed that the blue-shift has been induced by both the decrease in the amount of indium in the core and the quantum confinement effect, it is not definite whether the doping of zinc ion is an additional cause of blue-shift or not.

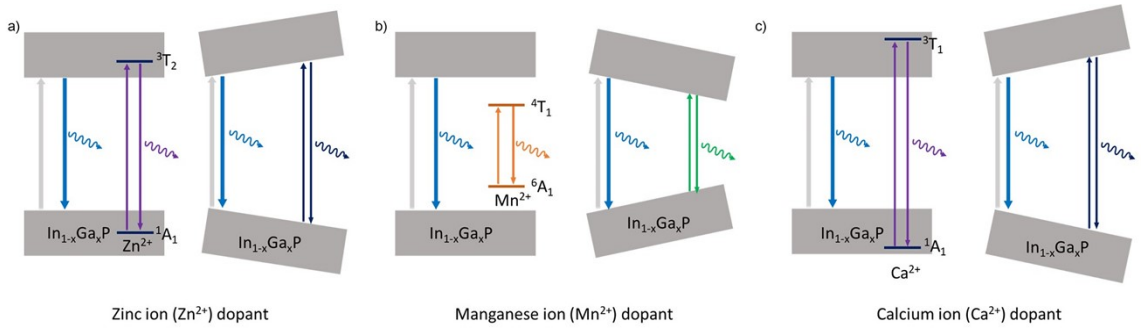

Fig. S2. Energy states of each dopants in $In_{1-x}Ga_xP$. Each includes two cases when the dopants are doped. Left, the case when the dopant insists on maintaining its own energy states. Right, the case when the dopant is assimilated with $In_{1-x}Ga_xP$ inducing the change in exciton energy following Vegard's Rule. (a) Zinc ion (Zn^{2+} dopant), (b) Manganese ion (Mn^{2+} dopant), and (c) Calcium ion (Ca^{2+} dopant)

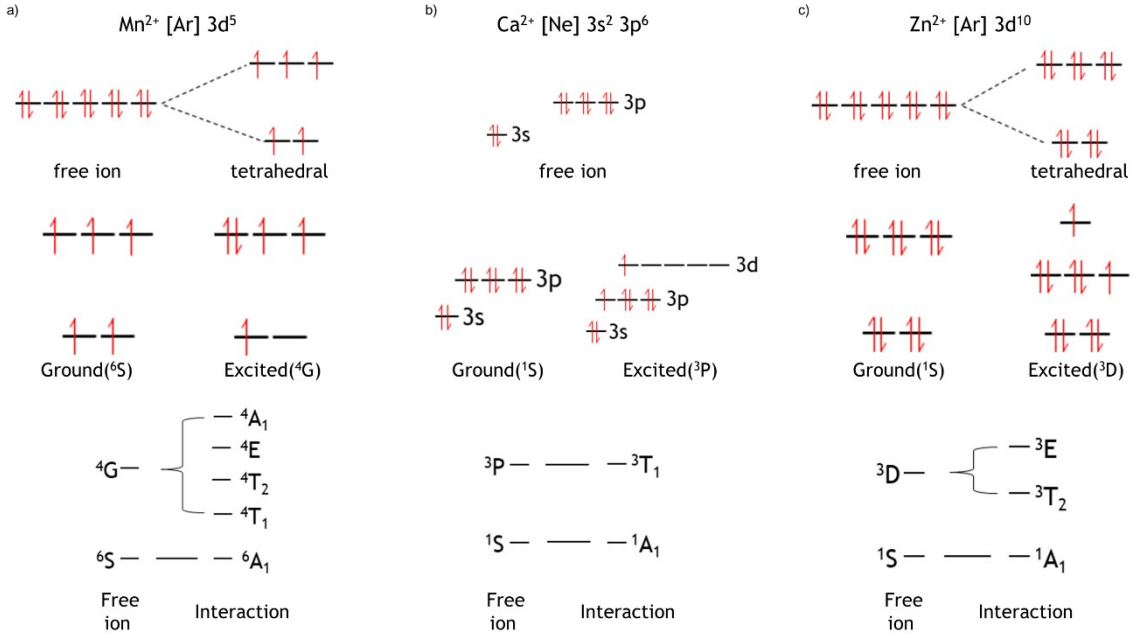

Fig. S3. Theoretical analysis on the first transition state of each ions: (a) manganese ion (Mn^{2+}) from $^6A_1$ to $^4T_1$, (b) calcium ion (Ca^{2+}) from $^1A_1$ to $^3T_1$, and (c) zinc ion (Zn^{2+}) from $^1A_1$ to $^3T_2$

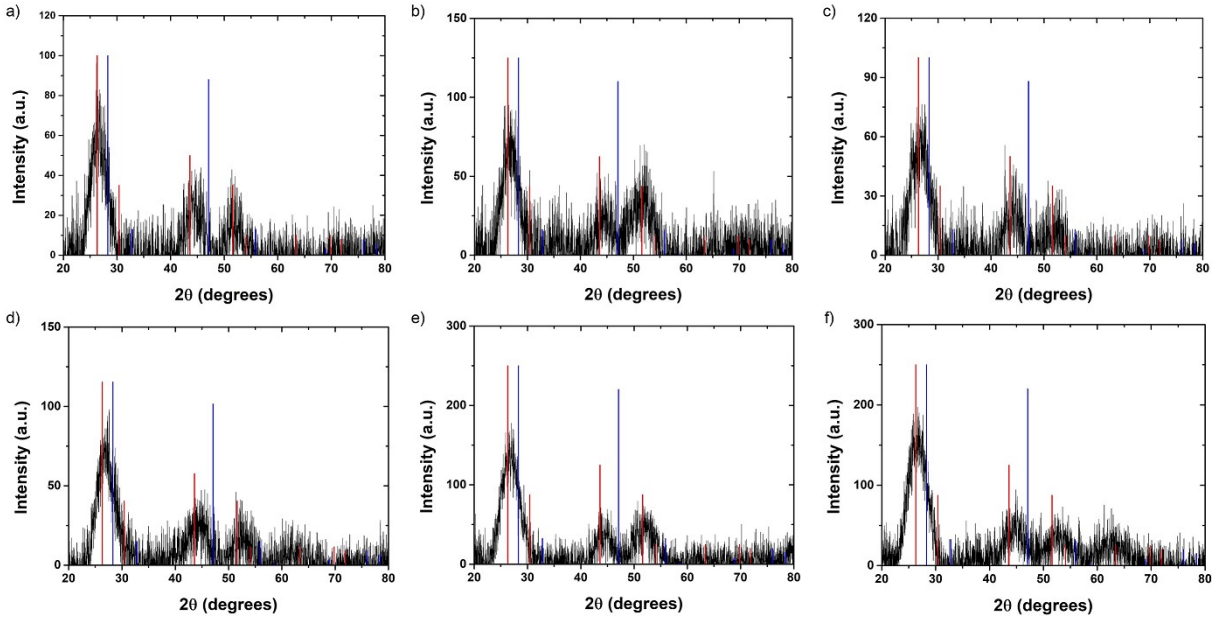

Fig. S4. XRD patterns of (a) MnCa0.5,0.5, (b) MnCa0.5,1, (c) MnCa1,1, (d) ZnCa0.5,0.5, (e) ZnCa0.5,1, and (f) ZnCa1,1. Colored lines are standard XRD pattern of InP (JCPDF: 032-0452, red line) and GaP (JCPDF: 032-0397, blue line).

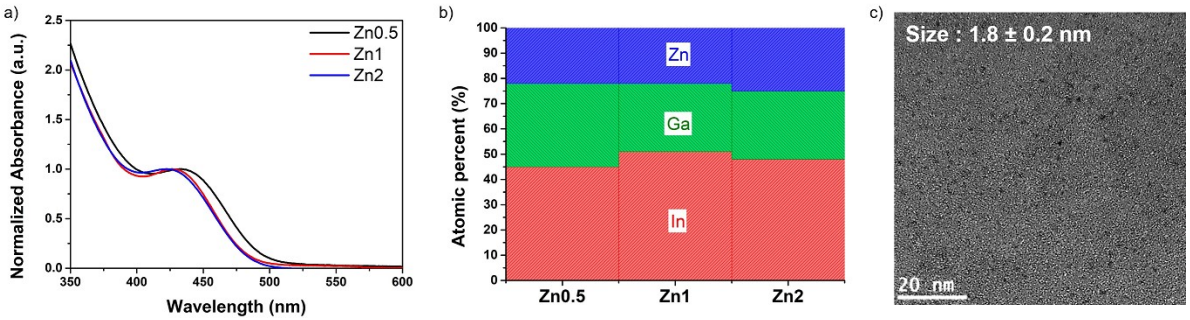

Fig. S5. (a) Absorption spectra and (b) graphical representation of ICP-AES data of Zn0.5, Zn1, and Zn2. (c) TEM image of Zn2 (scale bar: 20 nm)

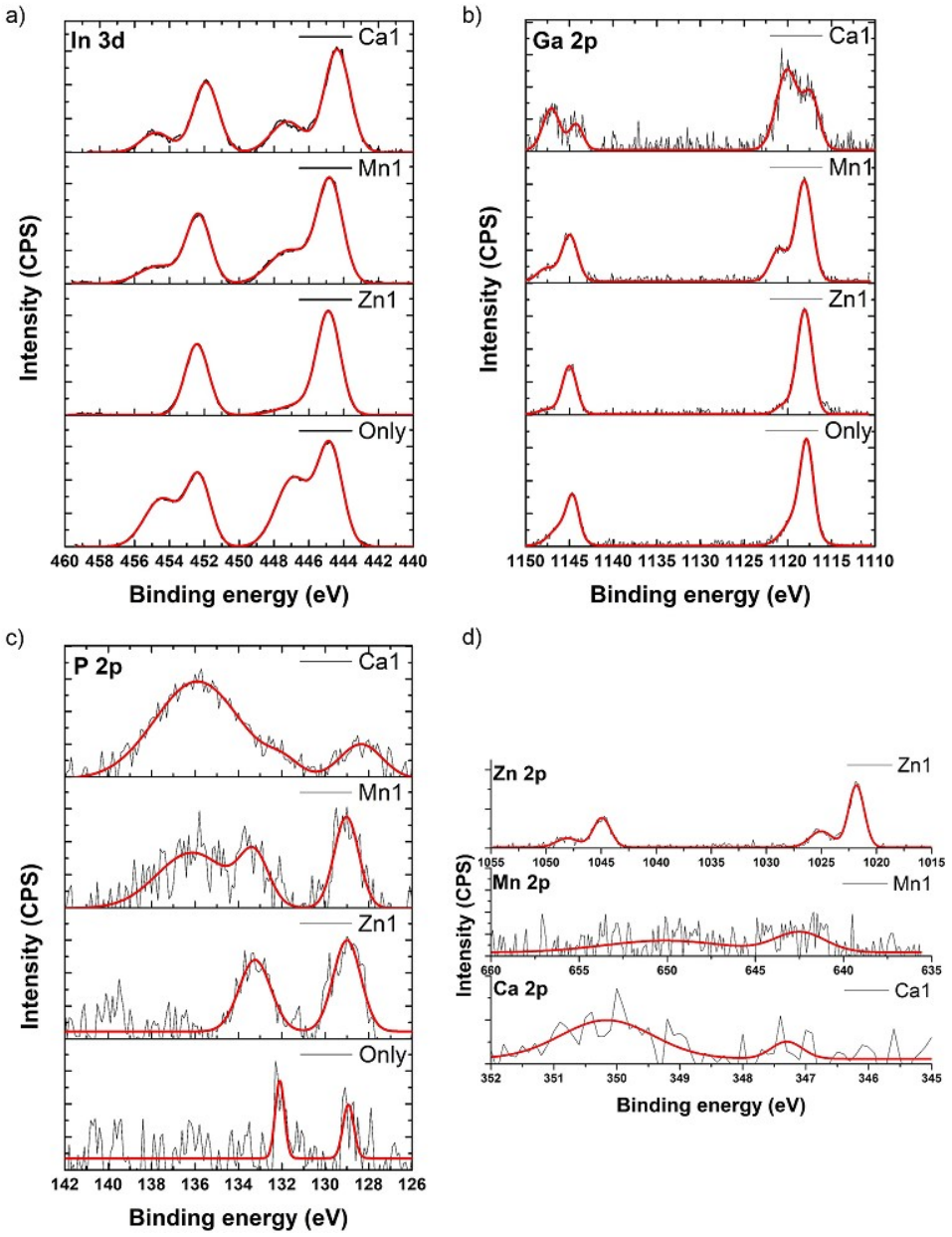

Fig. S6. XPS spectrum of Only, Zn1, Mn1, and Ca1 samples: (a) In 3d peaks, (b) Ga 2p peaks, (c) P 2p peaks, (d) Zn 2p peaks of Zn1, Mn 2p peaks of Mn1, and Ca 2p peaks of Ca1.

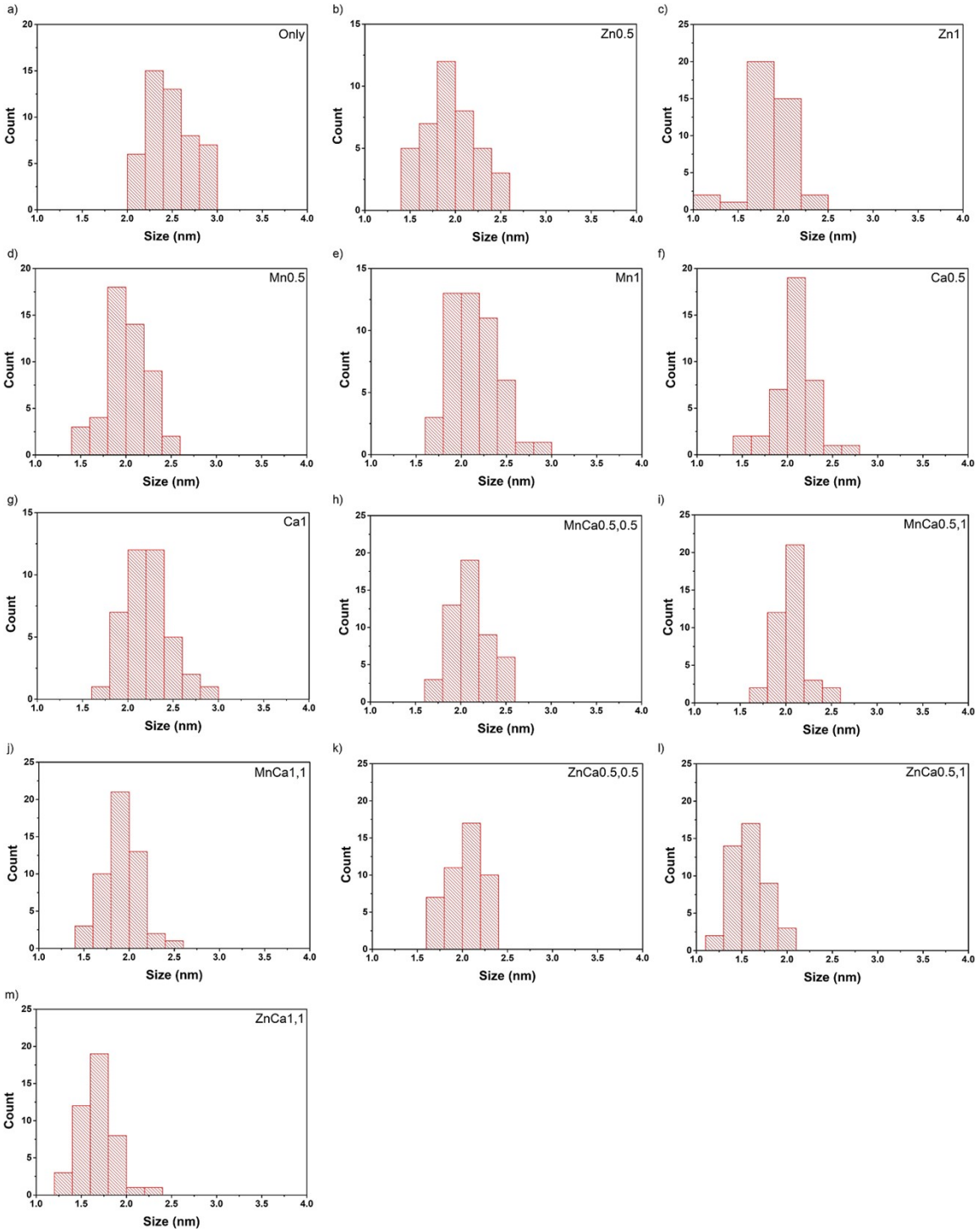

Fig. S7. Size distribution graphs based on ImageJ program: (a) Only, (b) Zn0.5, (c) Zn1, (d) Mn0.5, (e) Mn1, (f) Ca0.5, (g) Ca1, (h) MnCa0.5,0.5, (i) MnCa0.5,1, (j) MnCa1,1, (k) ZnCa0.5,0.5, (l) ZnCa0.5,1, and (m) ZnCa1,1

Table S1. Absolute hardness of metal ions used in the synthesis

	Zn^{2+}	Mn^{2+}	In^{3+}	Ga^{3+}	Ca^{2+}
Absolute hardness	11	9	13	17	20

Table S2. Summary of LEET, sizes, and the ratio of In and Ga of Zn0.5,0.5, Ca0.5, and MnCa0.5,0.5

	LEET (nm)	Size (nm)	In[a]	Ga[a]
ZnCa0.5,0.5	449	2.0 ± 0.2	0.82	0.18
Ca0.5	497	2.1 ± 0.2	0.79	0.21
MnCa0.5,0.5	488	2.1 ± 0.2	0.79	0.21

[a] X: the atomic ratio of metal X to (In+Ga)

Table S3. The LEET, sizes, and ICP-AES data on Zn0.5, Zn1, and Zn2

	LEET (nm)	Size (nm)	Including zinc			Excluding zinc	
			In[a]	Ga[a]	Zn[a]	In[b]	Ga[b]
Zn0.5	433	2.0 ± 0.3	0.45	0.33	0.22	0.57	0.43
Zn1	427	1.8 ± 0.3	0.51	0.27	0.22	0.65	0.35
Zn2	423	1.8 ± 0.2	0.48	0.27	0.25	0.64	0.36

[a]X: the atomic ratio of metal X to (In + Ga + Zn). [b]Y: the atomic ratio of metal X to (In + Ga)

References

S1. Y. Kim, K. Yang and S. Lee, *J. Mater. Chem. C*, 2020, **8**, 7679.

S2. M. Wei, J. Yang, Y. Yan, L. Yang, J. Cao, H. Fu, B. Wang and L. Fan, *Phys. E*, 2013, **52**, 144-149.

S3. W. Liu, Q. Lin, H. Li, K. Wu, I. Robel, J. M. Pietryga and V. I. Klimov, *J. Am. Chem. Soc.*, 2016, **138**, 14954-14961.

S4. A. Kramida, Ralchenko, Yu., Reader, J., and NIST ASD Team, *Journal*, 2020, DOI: https://doi.org/10.18434/T4W30F.

S5. G. Zhang, S. Mei, X. Wei, C. Wei, W. Yang, J. Zhu, W. Zhang and R. Guo, *Nanoscale Res. Lett.*, 2018, **13**, 170.

S6. H. Xu, J. Liang, Z. Zhang, Z. Deng, Y. Qiu, M. He, J. Wang, Y. Yang and C.-C. Chen, *RSC Adv.*, 2021, **11**, 2437-2445.